

Coherent control of frequency conversion toward short (picosecond) vacuum-ultraviolet radiation pulses

Holger Muench,^{*} Shrabana Chakrabarti, and Thomas Halfmann

Institute of Applied Physics, Technical University of Darmstadt, Hochschulstraße 6, D-64289 Darmstadt, Germany

(Received 2 June 2010; published 20 September 2010)

We present experimental data on the coherent control of frequency conversion toward the vacuum-ultraviolet regime in xenon atoms, applying intense ultrashort picoseconds (ps) radiation pulses. We report on quantum interference between two resonantly enhanced frequency conversion processes (i.e., fifth harmonic generation and four-wave mixing). The conversion processes are driven by a fundamental (ps) laser pulse at 530 nm and the phase-locked second harmonic at 265 nm. Both fifth harmonic generation and four-wave mixing yield vacuum-ultraviolet radiation at 106 nm. The two frequency conversion pathways interfere with each other—either constructively or destructively, depending on the relative phase of the driving laser pulses. Thus, by variation of the relative phase, we substantially enhance or reduce the conversion efficiency (i.e., the yield of generated vacuum-ultraviolet radiation).

DOI: [10.1103/PhysRevA.82.033821](https://doi.org/10.1103/PhysRevA.82.033821)

PACS number(s): 42.65.Ky, 32.80.Qk

I. INTRODUCTION

The generation of coherent radiation in the vacuum-ultraviolet (VUV) spectral regime is an active field of modern laser-based research. VUV radiation finds application in high-resolution microscopy, laser lithography, spectroscopy, and the generation of ultrashort radiation pulses toward the regime of attosecond pulse duration. Many of these applications require VUV radiation at ultrashort pulse durations. Resonantly enhanced frequency up-conversion, driven by intense laser pulses, exhibits an appropriate way to generate VUV pulses [1–3]. However, the conversion efficiencies in typical many-photon excitation schemes are usually rather small. Therefore, we require techniques to enhance the frequency conversion processes.

Concepts, based on quantum interference or coherent control, offer possibilities to achieve this goal. Coherent control relies on the interference between simultaneous excitation pathways from an initial quantum state to a target quantum state. As a specific control scenario, here we mention techniques based on “phase control” [4]. By variation of the relative phase between the excitation pathways (i.e., the driving laser fields) we get constructive or destructive interference. This permits the enhancement or suppression of the total excitation probability. Phase control (or coherent control) was applied to a variety of excitation schemes, processes, and media [4]. Most experiments aimed at the control of atomic or molecular populations (i.e., excitations to bound states or continuum states). The latter corresponds to control of photoionization and photodissociation yields. There are only very few experiments dealing with coherent control of frequency conversion [5–7].

Also coherent control of frequency conversion processes relies on the interference of two frequency conversion pathways. We may implement this scheme by two simultaneous, but different frequency mixing processes in the same medium, generating the same output frequency. To apply techniques of phase control we require a constant phase relationship

between the driving radiation fields. Also here, the interference of the conversion processes is either constructive or destructive—depending on the relative phase of the two conversion pathways (i.e., the relative phase of the radiation fields).

In the following, we report experimental results on coherent control of resonantly enhanced frequency conversion toward the VUV regime, applying intense, short (ps) laser pulses. In contrast to the few previous investigations on phase control of frequency conversion, we apply intense, short laser pulses (rather than long nanosecond pulses [6,8]), generate shorter wavelengths, and also aim at higher-order frequency conversion processes. These features are of interest for future applications of quantum interferences in the field of ultrashort laser pulses (i.e., toward high-order harmonic generation and subfemtosecond radiation pulses at extreme-ultraviolet wavelengths).

II. COUPLING SCHEME AND EXPERIMENTAL SETUP

In our experiment we investigate coherent control of simultaneous fifth harmonic generation and four-wave mixing in a dense supersonic jet of xenon atoms (see Fig. 1). Xenon exhibits an efficient medium with large susceptibilities for frequency conversion toward short wavelengths. In our coupling scheme, both fifth harmonic generation and four-wave mixing are resonantly enhanced via a two-color three-photon transition or a one-color five-photon transition between the ground state $5p^6\ ^1S_0$ and the excited state $8d^2\ [1/2]_1$. We drive fifth harmonic generation by an intense short laser pulse at wavelength $\lambda_1 = 530$ nm. We drive four-wave mixing by one photon from the pulse at $\lambda_1 = 530$ nm and two photons at wavelength $\lambda_2 = 265$ nm. Both frequency conversion processes yield signal radiation at wavelength $\lambda_S = 106$ nm (i.e., deep inside the VUV regime). Obviously, in our coupling scheme the radiation at $\lambda_2 = 265$ nm is the second harmonic of the beam at $\lambda_1 = 530$ nm. Thus, the phases of the two beams are automatically locked to each other, provided we deduce the ultraviolet beam from the fundamental radiation by second harmonic generation. Moreover, also frequency jitter of the fundamental radiation does not play

^{*}holger.muench@physik.tu-darmstadt.de

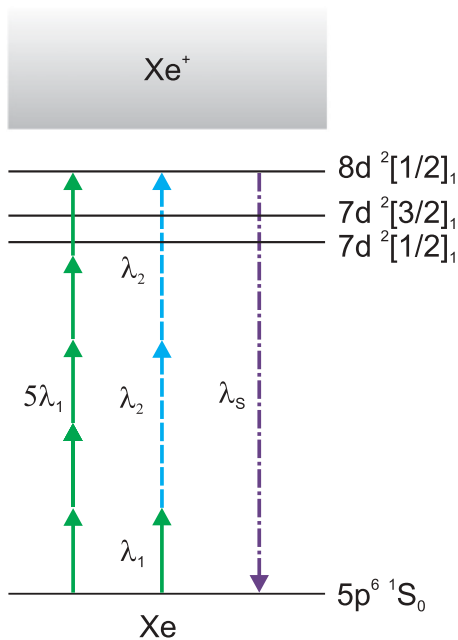


FIG. 1. (Color online) Coupling scheme with relevant energy levels.

a role in this configuration, and both pulses are perfectly synchronized. This enables us to manipulate the absolute yield of the generated radiation at 106 nm by a variation of the relative phase between the driving laser pulses under quite stable experimental conditions. We note that by tuning the laser wavelengths, we may alternatively also implement a coherent control scenario via other excited states (e.g., states $7d^2 [3/2]_1$ and $7d^2 [1/2]_1$, compare Fig. 1). In the following, we will further discuss conclusions from spectroscopic investigations on frequency conversion via alternative excited states.

We also note that frequency mixing processes involving an even number of photons (e.g., sum frequency mixing of three fundamental photons at wavelength λ_1 and one photon at wavelength λ_2) could yield VUV photons at our previous wavelength λ_s . However, selection rules for electric dipole transitions forbid conversion processes with an even number of photons in our coupling scheme. Conversion processes via higher-order multipole transitions are negligible.

The experimental setup is as follows (see Fig. 2): A titanium:sapphire oscillator (MIRA 900P, Coherent), pumped by a frequency doubled, continuous-wave Nd:YAG laser

(VERDI V18, Coherent), generates laser pulses with a pulse duration 1.2 ps (full width at half-maximum, FWHM) at a wavelength of 769 nm. The repetition rate of the pulse train is 76 MHz. The pulse train serves to synchronously pump an optical parametric oscillator (OPO) with intracavity frequency doubling (OPO automatic, APE GmbH), yielding tunable (ps) radiation pulses in the visible regime. A wavelength meter (Wavescan, APE GmbH) measures the wavelength of the generated pulses. The pulses are linearly polarized, with a pulse duration of 1.3 ps (FWHM) and spectral bandwidth close to the Fourier transform limit. The average output power is 300 mW, corresponding to pulse energies of 4 nJ, at a repetition rate of 76 MHz. The pulse train propagates into a three-stage dye amplifier chain, pumped by the third-harmonic frequency of a pulsed injection-seeded Nd:YAG laser (GCR4, QuantaRay/Spectra-Physics) at a repetition rate of 20 Hz. We synchronize the picosecond pulses from the OPO and the nanosecond pulses from the Nd:YAG pump laser by fast electronics, including a variable delay generator (DG535, SRS) as a major component. The pulse energy of the amplified (ps) pulses in the visible regime reaches $E_1 \approx 100 \mu\text{J}$. We note that the dye amplifier also acts as a pulse picker (i.e., it reduces the repetition rate of the pulse train to 20 Hz). We experimentally characterized the obtained, amplified pulses in a homemade third-order autocorrelator and spectrometer, applied for frequency-resolved optical gating (FROG). The amplified (ps) pulses are linearly polarized, with pulse duration $\tau_1 = 1.3$ ps, and spectral bandwidth close to the Fourier transform limit (i.e., $\Delta\lambda_1 = 0.4$ nm). For the experiments, discussed in the following, we tune the center wavelength of the OPO in the interval $\lambda_1 = 525\text{--}550$ nm.

We focus the (ps) pulses in a $\beta\text{-BaB}_2\text{O}_4$ (BBO) crystal to generate the second harmonic frequency at tunable, ultraviolet wavelengths in the interval $\lambda_2 = 263\text{--}275$ nm. The resulting laser pulses at fundamental and second harmonic frequency are orthogonally polarized. The pulse energy of the ultraviolet laser pulses is in the range of $E_2 = 5 \mu\text{J}$. From cross-correlation measurements, using the four-wave mixing scheme described previously, we deduce a pulse duration of $\tau_2 \approx 1$ ps. We apply a dielectric mirror to separate the fundamental and second harmonic beam and collimate the beams by additional lenses. The second harmonic laser beam propagates along an optical delay line to synchronize fundamental and second harmonic laser pulses. The fundamental laser beam passes an achromatic half-wave plate (HWP) to match the polarization direction with the second harmonic beam. The fundamental

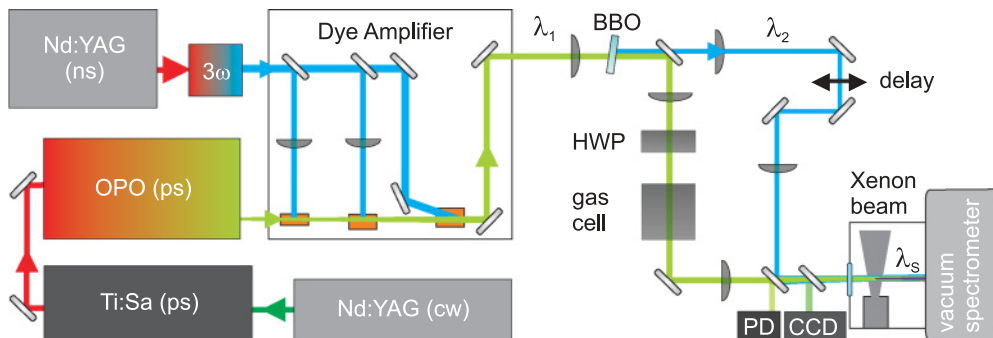


FIG. 2. (Color online) Experimental setup.

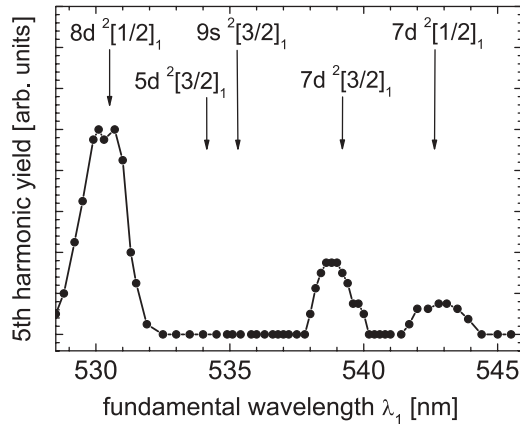


FIG. 3. Fifth harmonic yield vs. fundamental laser wavelength.

beam also propagates through a short gas cell (length 100 mm) filled with argon at adjustable pressure. This serves to vary the relative phase of the fundamental and second harmonic by variation of the argon pressure.

We focus the two beams independently (with lenses of focal length $f_1 = 100$ mm and $f_2 = 150$ mm), recombine them on a dielectric mirror and spatially as well as temporally overlap them in the interaction region (i.e., with the xenon jet inside a small vacuum chamber). The xenon jet is generated from a pulsed nozzle (General Valve, stagnation pressure 700 mbar, orifice diameter 0.8 mm). The laser beams intersect the atomic beam approximately 1 mm downstream. The diameters of the laser beams in the interaction region are $d_1 \approx 20$ μm (FWHM) for the fundamental beam and $d_2 \approx 50$ μm (FWHM) for the second harmonic beam. This yields intensities up to $I_1 = 3 \times 10^{13}$ W/cm² and $I_2 = 7 \times 10^{10}$ W/cm². We also estimated the confocal parameters of the beams and get $L_1 = 0.8$ mm and $L_2 = 20$ mm.

The two laser pulses simultaneously drive fifth harmonic generation and four-wave mixing in the xenon atoms (compare Fig. 1), yielding signal pulses in the interval $\lambda_2 = 105\text{--}110$ nm. The signal beam propagates collinearly with the fundamental and second harmonic beam into an evacuated spectrometer, equipped with a concave, reflective grating (VM502, ACTON Research, resolution $\Delta\lambda = 4$ nm). The spectrometer separates the signal beam and directs it onto an electron multiplier tube (EMT R595, Hamamatsu) for detection. The output signal of the electron multiplier is integrated by a boxcar gated integrator (SR250, SRS) and processed in a computer. To reduce the effect of intensity fluctuations in the highly nonlinear optical processes, we monitor the intensity of the fundamental laser pulse on a fast integrating photodiode (PDI-400, Becker & Hickl) and permit only laser shots in a small intensity window (typically 5% of the required intensity) during data collection. Moreover, we also monitored the spatial laser beam profiles on a UV-enhanced charge coupled device (CCD) camera to ensure stable beam geometry during data collection.

III. EXPERIMENTAL RESULTS AND DISCUSSION

In the following, first we present some spectroscopic data on resonantly enhanced fifth-harmonic generation in xenon. These data serve to determine and confirm appropriate

conditions for our coherent control experiment. Second, we discuss the main experimental results on coherent control (phase control) of frequency conversion processes toward the VUV regime.

The conversion efficiency of resonantly enhanced fifth harmonic generation depends on the effective multiphoton transition moment from the ground state $5p^6\ ^1S_0$ to an excited state in xenon. While single-photon transition moments are available from standard databases, there are almost no spectroscopic data on effective multiphoton transition moments (or nonlinear susceptibilities) for higher-order processes (e.g., fifth harmonic generation). Thus, we performed some simple nonlinear spectroscopy to determine the relative conversion efficiencies and phase-matching conditions for fifth harmonic generation in xenon. In particular, we measured the fifth harmonic yield versus wavelength λ_1 of the fundamental (ps) laser pulse, while the pulse at λ_2 was switched off (see Fig. 2). The laser intensity in the interaction region was $I_1 = 1 \times 10^{13}$ W/cm². To guarantee constant experimental conditions (e.g., beam overlap) during the measurement, we also monitored off-resonant third harmonic generation of the fundamental (ps) pulse in xenon. Due to the far off-resonant character of the process, the third harmonic yield is expected to remain constant during a wavelength scan. This served as an additional indicator for the stability of the beam geometry during a wavelength scan.

Figure 3 shows the fifth harmonic yield versus the fundamental laser wavelength λ_1 . The arrows and labels in the figure indicate the energetic positions of excited states, as taken from spectroscopic databases [9]. We identify the maxima of fifth harmonic yield at transitions from the ground state $5p^6\ ^1S_0$ to excited states $8d^2\ [1/2]_1$, $7d^2\ [3/2]_1$, and $7d^2\ [1/2]_1$. Two additional transitions, which should also appear in the tuning range, show no fifth harmonic signal above the noise level. We observe the largest resonance enhancement for the transition to state $8d^2\ [1/2]_1$. Thus, we decided to apply this transition in our coherent control experiment.

We note that the maxima of the observed peaks spectrally coincide well with the expected transition wavelengths. Moreover, the peaks are quite symmetric. These properties indicate negligible phase mismatch during the conversion process. This is due to the fact that the interaction length L in the atomic beam does not exceed the coherence length L_C of the frequency conversion process: The fundamental and generated radiations propagate at different phase velocities inside the nonlinear medium. The coherence length is here defined by a phase slip of 2π between the fundamental and generated radiation. In our case the phase mismatch per atom for sum frequency generation is on the order of $\Delta k/n \approx 10^{-16}$ cm² [1] with the total phase mismatch Δk and the gas density n . We assume a homogenous gas density distribution along the propagation axis of the laser pulses. For our interaction geometry we get a gas density of $n \approx 5 \times 10^{16}$ cm⁻³ [10]. From these values we calculate the coherence length for our conversion process $L_C = 2\pi/\Delta k \approx 1$ cm. The coherence length exceeds the interaction length by one order of magnitude.

In case of a larger interaction length, we would expect a shift of the maximal conversion yield with regard to the expected spectral position of the resonance. The maximum would shift toward the negative-dispersive side of the resonance, to provide

better phase-matching conditions along the larger extension of the interaction region [1,11,12]. Thus, the spectral line would experience a shift and an asymmetry. This is not the case in our spectrum. This confirms our conclusion to neglect the phase-matching effects in our coherent control experiment. We note that this is of particular importance for coherent control of any multicolor frequency conversion process. In a longer medium, we had to take different phase-matching conditions for fifth harmonic generation and four-wave mixing into account. These different conditions could cover the effects of a phase control experiment.

After the previous first investigations, we performed the experiment on coherent control (phase control) of frequency conversion processes in xenon. We tuned the wavelength of our laser system to $\lambda_1 = 530$ nm. The corresponding second harmonic wavelength was $\lambda_2 = 265$ nm. Both fifth harmonic generation and four-wave mixing generated VUV radiation pulses at $\lambda_S = 106$ nm. To obtain a strong modulation depth by coherent control, we require equal VUV signal intensities generated on both pathways. This is equivalent to match beam intensities in a conventional light interferometer to obtain maximal contrast. To avoid additional optics for attenuation, we adjusted the laser intensities by slight, controlled phase mismatch in the BBO crystal, which served to generate the second harmonic of the driving laser. In parallel, we monitored the spatial laser beam profiles on a UV-enhanced CCD camera to ensure stable conditions with regard to beam geometry and beam profiles, also when slightly changing the tilt angle of the BBO crystal.

To modulate the relative phase between the two driving laser pulses, we varied the pressure p_{Ar} in the argon cell, which was placed in the path of the fundamental laser beam (see Fig. 2). The fundamental laser radiation at λ_1 gains an additional phase $\varphi \propto \Delta p_{Ar}$, with respect to the second harmonic at λ_2 . We note that the fundamental beam participates both in fifth harmonic generation, as well as in four-wave mixing (see Fig. 1). However, the number of absorbed photons from the fundamental beam in the two processes is different. Therefore, when changing the relative phase of the fundamental beam by φ , we vary the relative phase of the two conversion processes by 4φ .

We calculate the absolute phase shift φ in the fundamental laser pulse according to $\varphi = 2\pi \frac{L}{\lambda} \frac{(n_0-1)}{p_0} \Delta p_{Ar}$ with the cell length $L = 10$ cm, the refractive index $n_0 = 1.000281$, at pressure $p_0 = 1013$ mbar and wavelengths close to λ_1 (i.e., for the sodium *D* line at 589 nm).

Figure 4 shows the VUV signal intensity versus the argon pressure or the calculated relative phase 4φ . The solid triangles show single-shot data (i.e., without any averaging). The solid, red line indicates the result of a Savitzky-Golay averaging algorithm, involving 200 points from the single-shot experimental data. To reduce signal fluctuations, we monitored the driving laser pulse energy with a photodiode and acquired data only for energies in a range of $\pm 3\%$ around a selected pulse energy. The remaining noise in the experimental data is mainly due to mechanical vibrations in the beam geometry, which give rise to phase jitter.

Already the single-shot experimental data clearly show an oscillation of the VUV yield with the argon pressure (i.e., the relative phase between the laser pulses). This oscillation

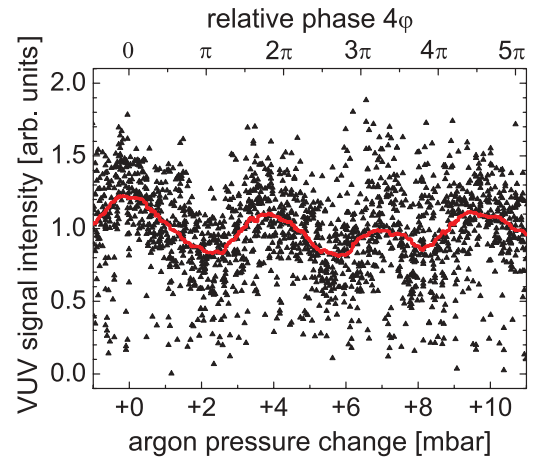


FIG. 4. (Color online) VUV signal intensity vs. argon pressure or phase shift 4 between the conversion pathways. Solid triangles depict single-shot data. The solid, red line indicates averaged data.

becomes quite pronounced in the averaged data. The two interfering frequency conversion pathways of fifth harmonic generation and four-wave mixing yield an overall VUV intensity $I_{\text{tot}} = I_A + I_B + 2\sqrt{I_A I_B} \cos(4\varphi)$, with the single VUV intensities I_A and I_B generated by fifth harmonic generation or four-wave mixing alone. 4φ is the absolute phase shift between the two interfering processes. The maximum total VUV intensity $I_{\text{max}} = I_A + I_B + 2\sqrt{I_A I_B}$ at a phase shift $4\varphi = k2\pi$, $k \in \mathbb{N}$, and the minimum total VUV intensity $I_{\text{min}} = I_A + I_B - 2\sqrt{I_A I_B}$ at a phase shift $4\varphi = (2k + 1)\pi$, $k \in \mathbb{N}$, depend on the ratio I_A/I_B . The contrast in the averaged interference pattern in Fig. 4, in the range of the first oscillation period, is defined by $K = (I_{\text{max}} - I_{\text{min}})/(I_{\text{max}} + I_{\text{min}})$, yielding $K \approx 20\%$. The single-shot data even indicate a contrast of $K \approx 45\%$. We do not reach the maximal contrast of 100% due to the following reasons: As discussed previously, intensity matching of the two conversion pathways exhibits a major issue in the experiment. This is quite difficult for nonlinear optical processes, also involving fluctuations. We also note that the previous considerations with regard to the total VUV intensity hold true only in the approximation of plane waves. For focused Gaussian beams, a contrast of 100% requires equal phase fronts of fundamental and second harmonic beams in the interaction region. This was not possible in our experimental geometry. Thus, though we did not reach the maximal contrast, the obtained, averaged modulation depth $K \approx 20\%$ exhibits a very good value.

We note that up to a calculated relative phase shift of $4\varphi = 2\pi$ our data also coincide quantitatively nicely with the expected behavior (i.e., a full oscillation period in the VUV yield). For larger phase shifts the oscillations seem to become slightly faster. This is probably due to the fact that we calculated the phase shift in the fundamental pulse, using the refractive index of argon at the sodium *D* line at 589 nm (which was the closest available wavelength from databases). Moreover, at larger pressure we might get an inhomogeneous gas density inside the cell, which could also change the expected phase shift.

Nevertheless, the previous experimental data clearly demonstrate the possibilities of coherent control (phase

control) to manipulate frequency conversion; also involving short laser pulses, higher-order conversion processes, and the generation of radiation toward very short wavelengths. The data encourage future investigation at even shorter wavelengths, shorter pulse duration, or improved conditions of phase matching (e.g., in a hollow-core, gas-filled fiber).

IV. CONCLUSION

We successfully demonstrated experimental implementation of coherent control (phase control) of frequency conversion processes, involving short (ps) laser pulses, aiming at the generation of VUV radiation. A fundamental (ps) laser pulse at $\lambda_1 = 530$ nm and its second harmonic at $\lambda_2 = 265$ nm simultaneously drive fifth-harmonic generation and four-wave mixing in a dense, supersonic jet of xenon atoms, yielding VUV radiation at $\lambda_S = 106$ nm. Both conversion processes are resonantly enhanced due to a multiphoton resonance between the ground state $5p^6\ ^1S_0$ and the excited state $8d^2[1/2]_1$ in xenon. By spectroscopic measurements, we confirmed appropriate phase-matching conditions for the experiment (i.e., negligible phase-matching effects in our geometry). We

modulate the phase of the fundamental laser pulse (i.e., also the relative phase between the two driving radiation pulses) in an argon cell with variable pressure. The phase modulation serves to manipulate the quantum interference between the two simultaneous frequency conversion processes, yielding a pronounced oscillation of the VUV yield versus argon pressure. We observed several, clearly visible cycles of oscillations, with a contrast of $K \approx 20\%$. Thus, by appropriate choice of the relative phase between the driving (ps) laser pulses (while keeping all other experimental parameters, e.g., pulse intensities, constant), the VUV yield increased or decreased substantially. The data clearly demonstrate the typical characteristics and potential of coherent control (phase control) scenarios, applied toward short laser pulses, frequency conversion processes, and the generation of radiation at short wavelengths.

ACKNOWLEDGMENTS

We acknowledge most valuable discussions with L. P. Yatsenko (National Academy of Sciences, Kiev/Ukraine), as well as financial support by the Deutsche Forschungsgemeinschaft (DFG).

-
- [1] G. Hilber, A. Lago, and R. Wallenstein, *J. Opt. Soc. Am. B* **4**, 1753 (1987).
 - [2] A. Tünnermann, K. Mossavi, and B. Wellegehausen, *Phys. Rev. A* **46**, 2707 (1992).
 - [3] H. Fielding, *Opt. Commun.* **123**, 129 (1996).
 - [4] M. Shapiro and P. Brumer, *Phys. Rep.* **425**, 195 (2006).
 - [5] N. E. Karapanagioti, D. Xenakis, D. Charalambidis, and C. Fotakis, *J. Phys. B* **29**, 3599 (1996).
 - [6] D. Xenakis, *Opt. Commun.* **152**, 83 (1998).
 - [7] E. Papastathopoulos, D. Xenakis, and D. Charalambidis, *Phys. Rev. A* **59**, 4840 (1999).
 - [8] X. Xing, D. Charalambidis, E. Koutsourelaki, and C. Fotakis, *Phys. Rev. A* **47**, 2296 (1993).
 - [9] Yu. Ralchenko, A. E. Kramida, J. Reader, and NIST ASD TEAM, NIST Atomic Spectra Database (National Institute of Standards and Technology, Gaithersburg, MD, 2010), version 3.1.5, [<http://physics.nist.gov/asd3>].
 - [10] T. Adachi, K. Kondo, and S. Watanabe, *Appl. Phys. B* **55**, 323 (1992).
 - [11] A. Lago, G. Hilber, and R. Wallenstein, *Phys. Rev. A* **36**, 3827 (1987).
 - [12] V. Peet, *Opt. Commun.* **189**, 267 (2001).